Fig. 3 *Predicted and measured power distribution for 126 mm focal length array at 10 GHz*
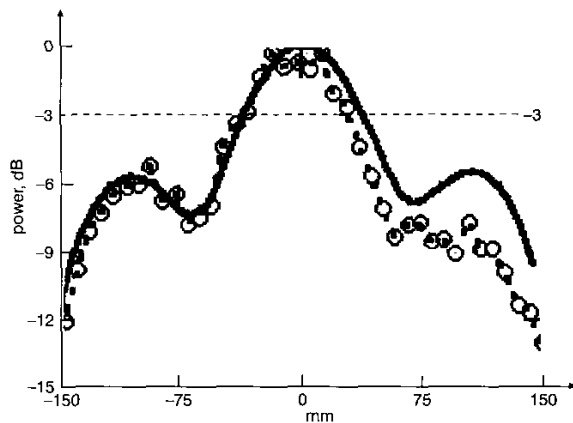
————predicted
- -O- -measured

Fig. 4 *Predicted and measured power distribution for 300 mm focal length array at 10 GHz*

————predicted
- -O- -measured

The new antenna has a significant size advantage over the previous focused beam solutions. For example, the same beam waist size was obtained with the 150 × 150 mm antenna array described here as that obtained with a spherical lens with 200 mm diameter illuminated by a standard X band horn antenna. In addition, the antenna array with a focused beam has a potential to provide advanced sensing options for microwave inspection applications.

M. Bogosanovich (*Industrial Research Ltd, PO Box 2225 Parnell, Auckland, New Zealand*)

E-mail: m.bogosanovich@irl.cri.nz

A.G. Williamson (*Department of Electrical and Electronic Engineering, The University of Auckland, Private Bag 92019, Auckland, New Zealand*)

References

1 BOGOSANOVIC, M., WILLIAMSON, A.G., THAKUR, K.P., HOLMES, W.S., and CRESSWELL, K.J.: 'A comparison of the systems for non-contact and non-destructive natural product inspection', 5th ISEMA Conf., Rotorua, New Zealand, March 2003 (accepted for publication)

2 BOGOSANOVIC, M.: New Zealand Patent Application No. 521823, October 2002

3 GOODMAN, J.W.: 'Introduction to Fourier optics' (Academic, New York, 1982)

4 HUYNH, T., and LEE, K.F.: 'Single-layer single-patch wideband microstrip antenna', *Electron. Lett.*, 1995, **31**, (16), pp. 1310–1312

5 POZAR, D.M.: 'Microwave engineering' (Addison-Wesley, 1990)

Exact representation of antenna system diversity performance from input parameter description

S. Blanch, J. Romeu and I. Corbella

A simple formulation to compute the envelope correlation of an antenna diversity system is derived. It is shown how to compute the envelope correlation from the S-parameter description of the antenna system. This approach has the advantage that it does not require the computation nor the measurement of the radiation pattern of the antenna system. It also offers the advantage of providing a clear understanding of the effects of mutual coupling and input match on the diversity performance of the antenna system.

Introduction: Antenna diversity is acknowledged as one of the techniques to increase spectrum efficiency in mobile communication systems. It is also recognised that mutual coupling of the antenna degrades the performance of a diversity antenna system. Therefore antenna designers try to design antenna systems that minimise coupling between ports while meeting the input matching requirements. Following [1] the envelope correlation for a two-antenna system is computed as:

$$\rho_e = \frac{\left|\iint_{4\pi}[\vec{F}_1(\theta,\phi)\bullet\vec{F}_2(\theta,\phi)]d\Omega\right|^2}{\iint_{4\pi}\left|\vec{F}_1(\theta,\phi)\right|^2 d\Omega \iint_{4\pi}\left|\vec{F}_2(\theta,\phi)\right|^2 d\Omega} \tag{1}$$

where $\vec{F}_i(\theta,\phi)$ is the field radiation pattern of the antenna system when port i is excited, and $\bullet$ denotes the Hermitian product. To compute (1) it is necessary to know the radiation pattern of the antenna system and perform the numerical integrations. This is a cumbersome process, whether it is done numerically or experimentally. Nevertheless this is the approach that is followed by most antenna designers [2, 3]. In [4] it is experimentally shown that the diversity antenna system performance can be determined from (1), mutual coupling measurements or direct envelope correlation measurement. In the following Section an exact expression to compute (1) from the S-parameter characterisation of the antenna system will be derived. This approach has the advantage that it is not necessary to know the radiation pattern of the antenna system, and that the explicit influence of mutual coupling and input match is revealed.
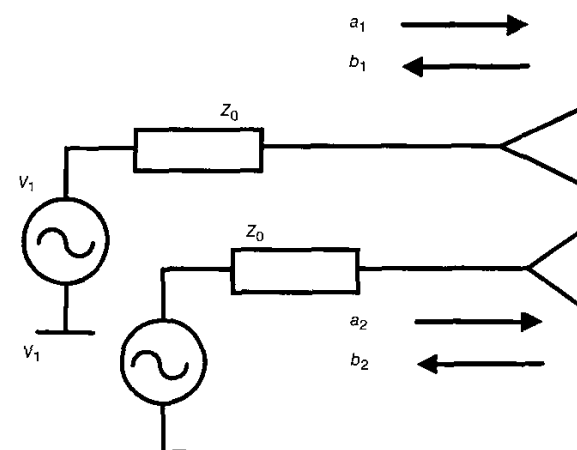

Fig. 1 *General geometry for two-antenna diversity system*

Mathematical derivation: Consider the situation shown in Fig. 1 in which two antennas are driven by two generators at the same frequency. The antennas are not necessarily well matched and have nonzero mutual coupling. For a given point at co-ordinates (r, θ, ϕ) in the far-field region, the total radiated electric field is the sum of the contributions from each antenna:

$$\vec{E} = \vec{E}_1 + \vec{E}_2$$

$$= a_1 \sqrt{\eta} \sqrt{\frac{D_1}{4\pi}} \vec{F}_1(\theta, \phi) \frac{e^{-jkr}}{r} + a_2 \sqrt{\eta} \sqrt{\frac{D_2}{4\pi}} \vec{F}_2(\theta, \phi) \frac{e^{-jkr}}{r} \quad (2)$$

where η is the free-space wave impedance, k the wave number, D_i the maximum directivity of antenna i and $\vec{F}_i(\theta, \phi)$ its normalised complex voltage pattern, which includes the effect of the other antenna terminated by the reference impedance Z_0. Note that both patterns are referred to a common co-ordinate system and are defined in terms of the incident wave (a_1 and a_2, respectively).

The total power radiated by both antennas is the integral of the power density over the whole space

$$P = \frac{1}{\eta} \iint_{\text{all space}} |\vec{E}|^2 \, dS$$

$$= \frac{1}{\eta} \iint_{\text{all space}} (|\vec{E}_1|^2 + |\vec{E}_2|^2 + \vec{E}_1 \bullet \vec{E}_2 + \vec{E}_2 \bullet \vec{E}_1) \, dS \quad (3)$$

which, using (2), can be written as:

$$P = |a_1|^2 C_{11} + |a_2|^2 C_{22} + C_{12} a_1 a_2^* + C_{21} a_2 a_1^* \quad (4)$$

being

$$C_{ii} = \frac{D_i}{4\pi} \iint_{4\pi} |\vec{F}_i(\theta, \phi)|^2 \, d\Omega \quad (5)$$

$$C_{ij} = \frac{\sqrt{D_i D_j}}{4\pi} \iint_{4\pi} (\vec{F}_i(\theta, \phi) \bullet \vec{F}_j(\theta, \phi)) \, d\Omega \quad (6)$$

for $i, j = 1$ or 2. In these equations, the differential solid angle $d\Omega = dS/r^2$ is used. From the definition of the scalar product, it follows that $C_{ij} = C_{ji}^*$. Equation (4) can be written in a more compact form as:

$$P = \mathbf{a}^+ \mathbf{C} \mathbf{a} \quad (7)$$

where $\mathbf{a}$ is the column vector of a_1 and a_2 and $\mathbf{C}$ is a 2×2 correlation matrix having (5) and (6) as elements.

However, the radiated power should be equal to the total power entering the two antennas. From S-parameter theory, this is:

$$P = \sum_{i=1}^{2} a_i - \sum_{i=1}^{2} b_i = \mathbf{a}^+ \mathbf{a} - \mathbf{b}^+ \mathbf{b} = \mathbf{a}^+ (\mathbf{I} - \mathbf{S}^+ \mathbf{S}) \mathbf{a} \quad (8)$$

being $\mathbf{I}$ the identity matrix and $\mathbf{S}$ the S-parameters defined in the input ports of the antennas. The symbol '$+$' indicates Hermitian transpose operation. Identifying this with (7), it follows that $\mathbf{C} = \mathbf{I} - \mathbf{S}^+ \mathbf{S}$ which is equivalent to the two following conditions:

$$\frac{D_1}{4\pi} \iint_{4\pi} |F_1(\theta, \phi)|^2 d\Omega = 1 - (|S_{11}|^2 + |S_{21}|^2) \quad (9)$$

$$\frac{\sqrt{D_1 D_2}}{4\pi} \iint_{4\pi} (\vec{F}_1(\theta, \phi) \bullet \vec{F}_2(\theta, \phi)) d\Omega = -(S_{11}^* S_{12} + S_{21}^* S_{22}) \quad (10)$$

Therefore by considering (9) and (10) the envelope correlation given by (1) can be expressed in terms of the S-parameters of the antenna system as:

$$\rho_e = \frac{|S_{11}^* S_{12} + S_{21}^* S_{22}|^2}{(1 - (|S_{11}|^2 + |S_{21}|^2))(1 - (|S_{22}|^2 + |S_{12}|^2))} \quad (11)$$

Application: As an example application, the envelope correlation for a two-antenna system formed by two collinear half-have dipoles has been computed following (1) and (11). In Fig. 2 the results obtained by both methods are shown against the spacing between antennas. The

antenna system input parameters and radiation patterns have been computed using MoM. It is clearly seen that both methods provide exactly the same result. It is also interesting to note that mutual coupling alone does not provide a good estimate for the envelope correlation. Another simple application of (11) is to evaluate the envelope correlation against operating frequency. In Fig. 3 the envelope correlation and the S-parameters for an orthogonal-fed square microstrip patch antenna is shown against frequency. Note that by using (11) the envelope correlation computation is straightforward from numerical simulation or laboratory measurement. On the contrary, the evaluation using (1) implies the computation or the measurement of the radiation patterns at each frequency.
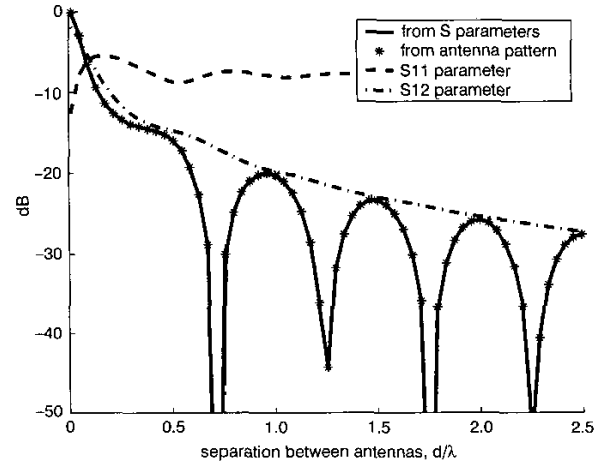

Fig. 2 *Envelope correlation and S-parameters for two collinear half-wave dipoles against their separation*
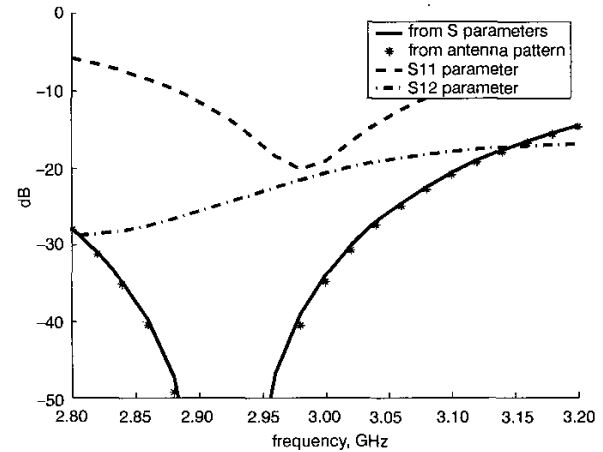

Fig. 3 *Envelope correlation and S-parameters for orthogonal-fed square microstrip patch antenna against frequency*

Conclusion: The expression that has been derived can be applied to compute the envelope correlation of any two-port antenna diversity system. It provides a simple functional to be minimised in an optimisation procedure design. It also shows that a certain set of simultaneous specifications such as mutual coupling, input match and cross-polar radiation may be redundant and in certain cases incompatible. Finally, this expression provides clear criteria in antenna design for minimising the envelope correlation. The expression can be easily extended to a multiple port antenna system, and can be applied in designing and assessing the diversity performance of antennas in mobile communications and remote sensing.

S. Blanch, J. Romeu and I. Corbella (*Electromagnetics & Photonics Engineering Group, Department of Signal Theory and Communications, Universitat Politecnica de Catalunya, c/Jordi Girona, 1-3, Mòdul D3, Campus Nord UPC, 08034 Barcelona, Spain*)

E-mail: romeu@tsc.upc.es.es

S. Blanch, J. Romeu and I. Corbella: Also with the Centre de Tecnologia de Telecomunicacions de Catalunya (CTTC)

References

1 VAUGHAN, R.G., and ANDERSEN, J.B.: 'Antenna diversity in mobile communications', *IEEE Trans. Veh. Technol.*, 1987, **36**, pp. 149–172
2 DIETRICH, C.B., DIETZE, K., NEALY, R.J., and STUTZMAN, W.L.: 'Spatial, polarization and pattern diversity for wireless handheld terminals', *IEEE Trans. Antennas Propag.*, 2001, **49**, pp. 1271–1281
3 JENSEN, M.A., and RAHMAT-SAMII, Y.: 'Performance analysis of antennas for hand-held transceivers using FDTD', *IEEE Trans. Antennas Propag.*, 1994, **42**, pp. 1106–1113
4 KO, S.C.K., and MURCH, R.D.: 'Compact integrated diversity antenna for wireless communications', *IEEE Trans. Antennas Propag.*, 2001, **49**, pp. 954–960

Uniplanar PBG screens for forming antenna patterns

C.R. Simovski and B. Sauviac

The possibility of forming the wideband 8-shaped pattern of an antenna in the *H*-plane with the use of a uniplanar photonic bandgap screen (UPPBGS) is studied. Two variants of UPPBGS are compared. The first is the known structure developed by the group of T. Itoh, the second is its suggested modification (presented by the authors). It is shown that the modified structure operates at lower frequencies than does the known structure (for the same cell size).

Introduction: In modern microwave techniques, printed circuit antennas are widely used. Generally these antennas are positioned on the interface of a dielectric layer with a metal ground plane. Often, one needs to make its thickness h very small compared to the wavelength λ in free space. To obtain constructive interaction of the antenna with the substrate and not to spend the greater part of energy in exciting the lateral waves in the dielectric, it is possible to use high-impedance surfaces (HIS). The HIS is usually thought of as a resonant magnetic wall (MW) with $h \ll \lambda/4$ [1].

A uniplanar photonic bandgap screen (UPPBGS) representing a complementing screen with respect to the grid of metal Jerusalem crosses (JC), which was suggested and studied by T. Itoh's group, found many applications. Of these, we consider the use of a UPPBG for shaping the antenna pattern. It is easy to prove that a planar perfectly conducting structure cannot behave as a HIS on its own. To have the properties of a HIS (MW) a UPPBGS must be associated with a metal ground plane. However, there are some cases when the structure should not be impenetrable. For example, the practical requirement can be to suppress the lateral radiation of the antenna, whereas the radiation is required in both upper and lower half-spaces (to form the 8-shaped pattern in the *H*-plane). In this case the UPPBGS can be applied alone since it suppresses the surface waves within rather wide frequency bands.

It was shown in [2] that the moderate inductive surface impedance $Z_s = jX_s$ (where $X_s > 0$ is the surface reactance) is preferable to divert the radiation of the horizontal antenna from the impedance plane over which the antenna is positioned. It concerns both the far-zone and near-zone of the antenna. When the surface reactance is high compared to the free-space impedance $X_s \gg \eta$ (the regime of MW), the total

radiation of the given antenna current is maximal, but lateral radiation is significant and the pattern in the *H*-plane is close to the semi-circle. When $X_s \sim \eta$, the total radiation is smaller but the lateral one is suppressed, and both near-field and far-field patterns are diverted from the plane [2]. In this Letter we show that the suppression of the lateral radiation holds also for a complex surface impedance (the real part of Z_s describes the transmission of the electromagnetic waves through the impedance surface). The main difference with the case of -the purely inductive Z_s (the case of HIS) is that the pattern is 8-shaped. To obtain this kind of pattern it is possible to use the known UPPBGS [3] as the impedance surface with complex surface impedance. In practice, suppressing the lateral waves is not sufficient for proper operation of the radiating system. It must be efficient, of course. Therefore, we need to obtain constructive interaction between the horizontal source and the UPPBGS. It is possible if X_s is positive and high enough with respect to the surface resistance R_s. Thus, there is a certain frequency band in which the UPPBGS [3] operates as required. Note, that the same consideration can be made for the source of TM-waves (vertical or horizontal magnetic antenna) when the required X_s is, in this case, negative (the case of a capacitive UPPBGS).
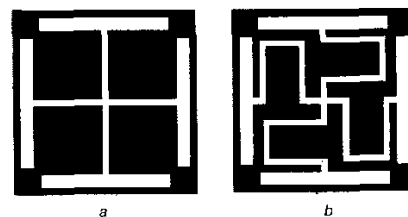

Fig. 1 *Unit cells*

a Unit cell of known structure (conventional JC)
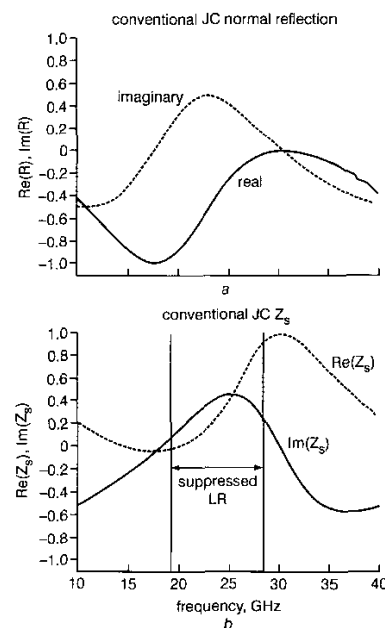*b* Unit cell of suggested structure (modified JC)

Fig. 2 *Reflection coefficient, and normalized surface impedance, for known UPPBGS [3]*

a Reflection coefficient   *b* Normalised surface impedance
—— Re(R)   —— Im($\hat{Z}_s$)
– – – Im(R)   – – – Re($\hat{Z}_s$)
Band in which lateral radiation is efficiently suppressed is shown

When the working frequencies are low, and the horizontal dimensions of the whole structure are restricted by a few centimetres, the use of UPPBGSs becomes difficult. In this situation, the required grid period turns out to be rather high and can be comparable with the